

EPOXY-EPOXY BIMATERIAL INTERFACE CRACKS IN ANNEALING RESIDUAL STRESSES

M.R. SHANBHAG, K. ESWARAN and P.B. GODBOLE

Corporate Research and Development, B.H.E.L. Vikasnagar,
Hyderabad 500 593, India

S.K. MAITI

Mechanical Engineering Department, I.I.T. Powai, Bombay 400 076, India

ABSTRACT

The possibility of initiation of interface cracks in the residual stress field after annealing a panel of dissimilar thermoplastics particularly near the edges is examined. The associated stress intensity factors for extension parallel to the interface and parallel debonding at the bond are also reported.

NOMENCLATURE

- σ_y - peel stress,
- σ_{xy} - shear stress
- σ_x - stress parallel to interface.
- h - thickness of the interface
- b, W - semilength, semiwidth of bimaterial panel respectively
- a - edge crack length
- $\Delta\alpha$ - difference in coefficients of linear thermal expansion
- E - modulus of elasticity
- p - push in pressure experienced by the adhesive film
- ν - Poisson's ratio
- ΔT - temperature trip during annealing operation

KEYWORDS: bimaterial, interface, residual stress, anneal, film

INTRODUCTION

Thin elastic films deposited on substrates often give rise to significant residual stresses in the film. The magnitudes of these stresses depend on the manufacturing process. If the film-substrate bonding is strong and the substrate is brittle a crack developed at the interface will divert into the substrate and attain a trajectory parallel to the interface [Fig.1]. The initiation of such cracks particularly near the edges and their initial growth have been studied by some investigators in terms of residual stress fields in the virgin system [Kao et.al, 1988]. Several experimental evidences pertaining to the extension of such cracks are presented by Suo and Hutchinson (1989). The objective of the present paper is to examine the possibility of origination of a crack at the edge of a bonded dissimilar pair of thermoplastics in the residual stresses reported in [5]. The subsequent course of extension and likely occurrence of parallel debonding are also studied. Some

results connected with experimentally observed geometry of the interface and SIFs too are presented.

RESULTS AND DISCUSSION

Annealing Residual Stress Fields

The geometry considered is shown in Fig. 2. Each solid of the bi-material panel is assumed to be homogeneous and linearly elastic. The interface is considered to be a smooth straight line without thickness for estimating stresses. The thermal mismatch residual stress fields were measured using photoelasticity and were computed using the finite element method after annealing the panel. These are detailed in [5]. The measured σ_x , σ_y and σ_{xy} stresses are reproduced in Figs. 3, 4 and 5 respectively for a panel made of thermoplastics CY230 and CT200 resins which are commonly used for photoelastic investigations. We restrict now our attention to a small edge region near the interface.

Thickness of Interface

Macroscopically the bondline can be taken as a line but microscopically this is not so. For the epoxy-epoxy and aluminium-epoxy material combinations considered in Ref. [5] the interface geometry was examined in an optical microscope (Reichert Austria) with 1:500 magnification. The observed bondline is schematically shown in Fig. 6. The average total height of wavy pattern for the 2 interfaces measured is 23 and 29 microns respectively. This is better than the bond thickness of 30-300 microns reported for adhesively sandwiched plates by Fleck et al, 1991.

Crack Tip Stresses

For a very short crack when the crack size is much smaller than the thickness attribute of the interface as defined in the above paragraph ($a/h \ll 1$) one may take the William's field still unperturbed at the crack tip. The stress field is completely parameterised by SIFs. These SIFs are,

$$\frac{K_I}{\sigma_0 \sqrt{h}} = 1.985 \frac{\sigma_y}{\sigma_0} \sqrt{\frac{a}{h}} \quad \dots \quad (1)$$

$$\frac{K_{II}}{\sigma_0 \sqrt{h}} = 1.985 \frac{\sigma_{xy}}{\sigma_0} \sqrt{\frac{a}{h}} \quad \dots \quad (2)$$

Therefore the two SIFs are in proportion of the residual peel (σ_y) and shear (σ_{xy}) stresses.

For a long crack ($a/h \gg 1$) extending from the edge upto about a tenth of the length of the bondline the residual peel stress on the interface and on lines parallel to it (macroscopically) is negative (Fig. 4). The residual shear stresses gradually diminish and become zero at the mid length of the interface ($x/2w = 0$) as shown in Fig. 5.

Since the peel stress is negative the edge crack will be subjected to compression perpendicular to its own plane. Hence it can not propagate further in mode I. This is in conformity with the observation reported in [2], wherein a ductile thin film is sandwiched between brittle substrates and the residual stresses in the film are simulated by loading shown in Fig. 7.

To substantiate the position let us consider some data. We consider the same bimaterial combinations as taken in [5]. The relevant material data are presented in Table 1. The constant σ_0 for the CY230-CT200 panel is 90 MPa. The variation of nondimensionalised SIFs with the crack length obtained through eqs. 1 and 2 for short cracks are shown in Figs. 8 and 9. For all the material combinations the bond line thickness is taken as 23 microns.

Effect of Large Residual Stress Parallel to the Bondline

We notice a near parabolic distribution of direct stress σ_x in the X direction on lines parallel (in macroscopic sense) to the interface (Fig. 3). This stress is zero on the bondline as given by Rice and Sih, 1965. At the edges it is zero and it has a peak at mid length of the interface. The average stress all along the bondline can be approximated after integration,

$$\frac{\sigma_x}{\sigma_0} \approx \frac{2}{3} \left(\frac{\sigma_x}{\sigma_0} \right)_{\max} \quad \dots \quad (3)$$

Fig. 10 depicts the actual and averaged values of this stress. This tensile residual stress can be thought of as an interface push-in pressure (Fig. 7).

Parallel Debonding

Considering the epoxy-epoxy interface at microscopic level and attributing a thickness parameter to it as done earlier we may consider the possibility of parallel debonding of the same as illustrated in Fig. 11. From Ref. [6] we have the scaling result for interface SIFs from the farfield results of SIFs for homogeneous substrate materials. As elaborated in that reference we shall consider Dundur's parameter β to be zero so that the oscillatory effects at the interface crack tip do not enter in our discussion. We use Irwin's formula relating energy release rate to SIFs at the upper crack tip (Fig. 11). As done in [8],

$$G = \frac{1-\nu^2}{E} [K_I^2 + K_{II}^2] \quad \dots \quad (4)$$

But we have under push-in pressure p , energy release rate to be

$$G = \frac{1-\nu^2}{E} \left(\frac{ph^2}{4} \right) \quad \dots \quad (5)$$

From eqns. 4 and 5 we have

$$K_I = \frac{1}{2} p \sqrt{h} \sin \phi \quad \dots \quad (6)$$

$$K_{II} = \frac{1}{2} p \sqrt{h} \cos \phi \quad \dots \quad (7)$$

After solving the full elasticity problem Ref.[8] gives $\phi=17.5$ degrees. We can draw qualitative conclusions about parallel debonding now. Since the stress is negative (residual tension) debonding will be in pure mode II sliding. It may be repeated here as in [8] that if this stress was positive (residual compression) a significant amount of crack face opening along with predominant sliding was possible. Hence in case of epoxy-epoxy interface parallel debonding is unlikely.

CONCLUSIONS

In a bimaterial panel subjected to annealing residual stresses, the mode I SIF at the tip of an edge crack close to the interface decreases with the edge crack length. But the trend shown by SIF for mode II is just the opposite. The SIF for mode I is the highest in the case of carbon-epoxy and mode II SIF is the largest for epoxy-epoxy material combinations. It appears that such extensions into the substrate very close to the interface are theoretically not feasible. In the case of an epoxy-epoxy interface, parallel debonding is also unlikely.

Acknowledgement: The authors thank the management of Bharat Heavy Electricals Limited at the Corporate Research and Development, Vikasnagar, Hyderabad, India for the kind permission to publish this work.

REFERENCES

1. Fleck, N.A., Hutchinson J.W. and Suo, Z. (1991). Crack path selection in a brittle adhesive layer, *Int. J. Solids Struc.*, 27 (3), 1683-1703.
2. Dao, H.C., Thouless, M.D. and Evans, A.G. (1986). Residual stresses and cracking in brittle solids bonded with a thin ductile layer, *Acta. Metall.*, 36 (8), 2037-2045.
3. Chiao, Y.H. and Clarke, D.R. (1990). Residual stress induced fracture in glass-sapphire composites - planar geometry, *Acta. Metall.*, 38, 251-258.
4. Rice, J.R. and Sih G.C. (1965). Plane problem of cracks in dissimilar media, *J. Appl. Mech.*, 32, 418-423.
5. Shanbhag, M.R., Maiti, S.K., Eswaran K. and Godbole P.B. (1991). Residual stresses in an epoxy - epoxy bi-material near interface due to annealing, B.H.E.L. (R&D) Technical Report, Hyderabad India.
6. Suo, Z. and Hutchinson, J.W. (1989). Sandwich test specimens for measuring interface crack toughness, *Mat. Sci. and Engng.*, A107, 135-143.
7. Suo, Z. and Hutchinson, J.W. (1989b). Steady state cracking in brittle substrates beneath adherent films, *Int. J. Solids Struc.*, 25, 1337-1353.
8. Suo, Z. (1990). Failure of brittle adhesive joints, paper S-279, *Appl. Mech. Rev.* 43(5), Part 2, Ed. C.F. Chen.

TABLE I
RELEVANT THERMOELASTIC PROPERTIES OF MATERIALS

MATERIAL	EY230 EPOXY	CT200 EPOXY	CARBON	KEVLAR49	ALUMINIUM	NYLON-66	E-GLASS
E, YOUNG'S MODULUS, GPa	3	3	300	125	70	1.6	76
POISSON'S RATIO	0.38	0.38	0.3	0.3	0.3	0.3	0.3
STRESS FRINGE CONSTANT N/N/FRINGE							
A. AT 30°C	8500	10000	-	-	-	-	-
B. AT 130°C	280	300	-	-	-	-	-
COEFFICIENT OF THERMAL EXPANSION $10^{-6}/^{\circ}\text{C}$	90	60	-0.5	-2	11	90	5

Epoxy resins, Hardeners have trade names of H/S Hindustan Ciba Belgij Ltd.

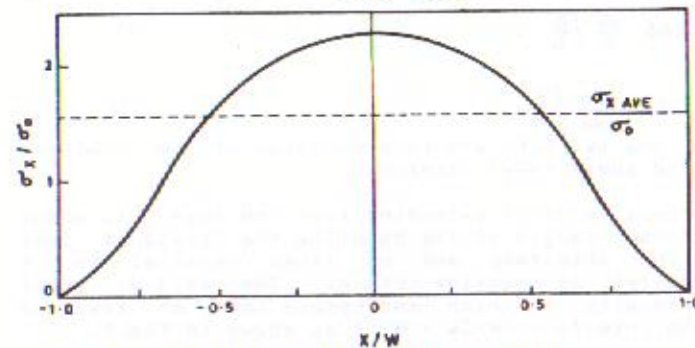
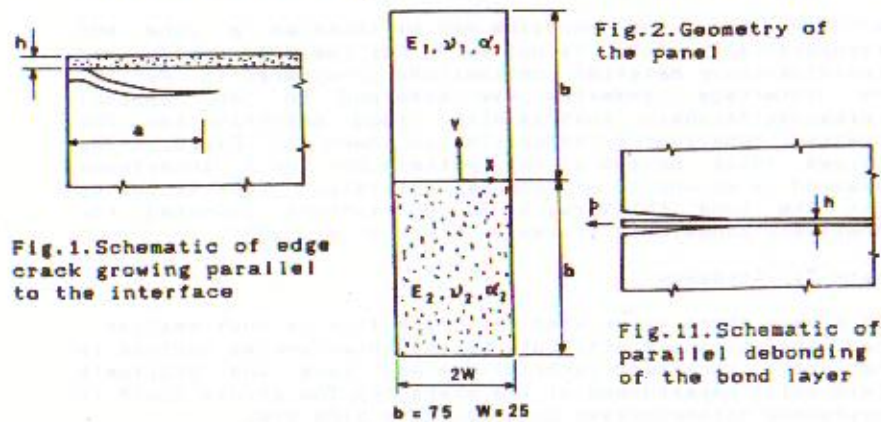


Fig. 10. Average residual σ_x stress

Note: Please see next pages for Figs. 3 to 9.

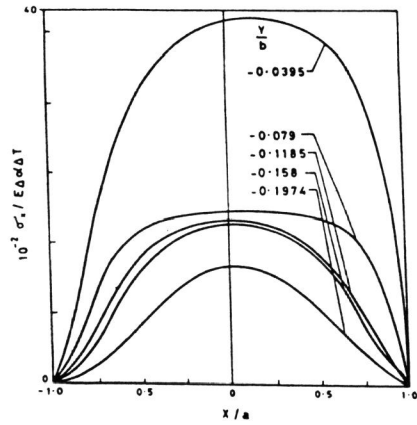


Fig. 3 Experimentally measured variation of σ_x with x for different y .

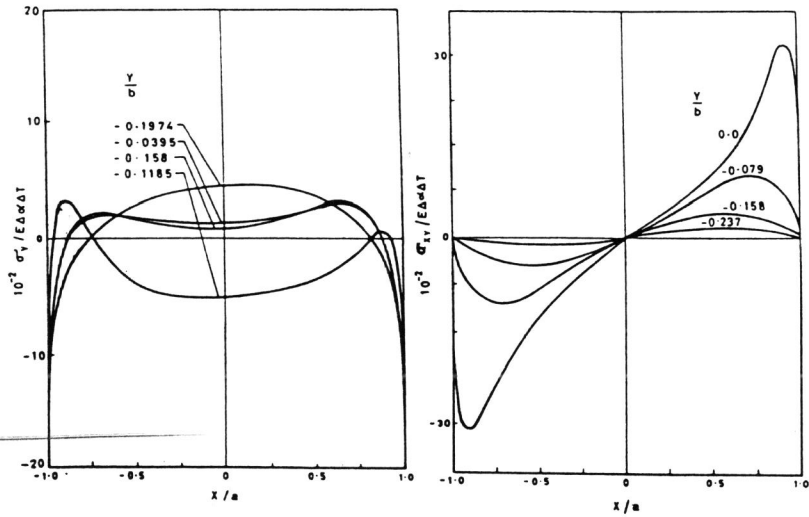


Fig. 4 Experimentally measured variation of σ_y with x for different y

Fig. 5 Experimentally measured variations of σ_{xy} with x for different y

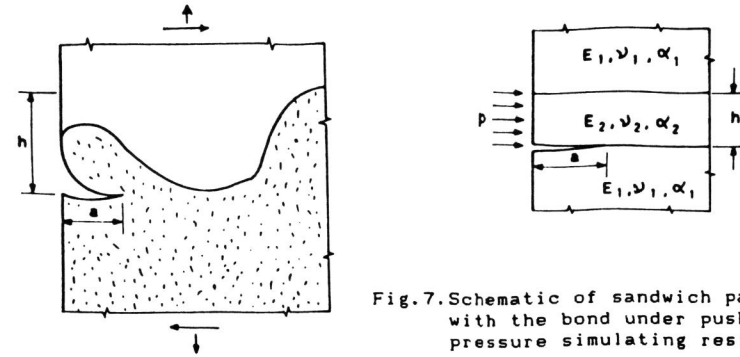


Fig. 7. Schematic of sandwich panel with the bond under pushin pressure simulating residual $\bar{\sigma}_x$

Fig. 6. Schematic of the interface as seen in an optical microscope

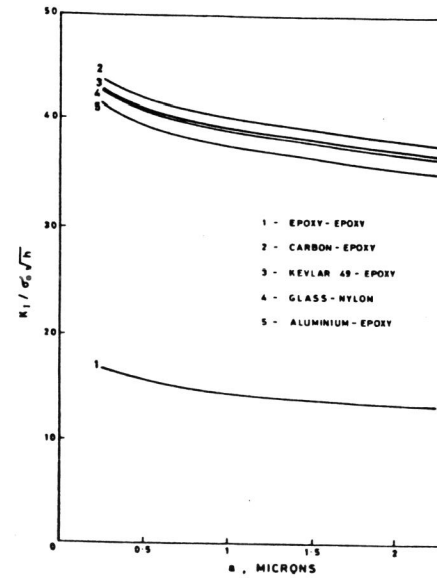


Fig. 8. Variation of K_I with the crack length

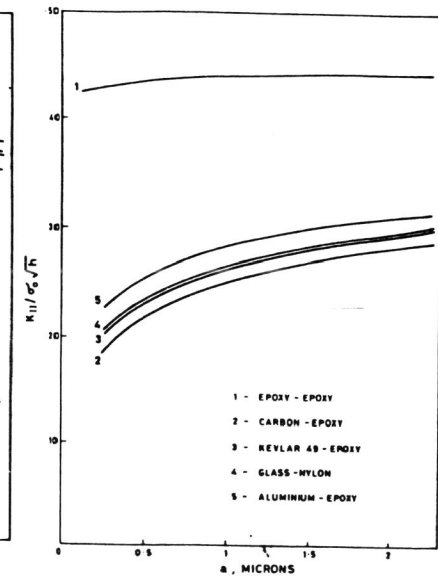


Fig. 9. Variation of K_{II} with the crack length